

UCLA

UCLA Electronic Theses and Dissertations

Title

Homogeneous Freestanding Luminescent Perovskite Organogel with Superior Water Stability

Permalink

<https://escholarship.org/uc/item/27s761xn>

Author

ZHANG, YUCHENG

Publication Date

2019

Peer reviewed|Thesis/dissertation

UNIVERSITY OF CALIFORNIA LOS ANGELES

**Homogeneous Freestanding Luminescent Perovskite Organogel
with Superior Water Stability**

A thesis submitted in the requirements for the degree Master of Science in
Materials Science and Engineering

by

Yucheng Zhang

2019

ABSTRACT OF THE THESIS

Homogeneous Freestanding Luminescent Perovskite Organogel with Superior Water Stability

by

Yucheng Zhang

Master of Science in Materials Science and Engineering

University of California, Los Angeles, 2019

Professor Ximin He, Chair

Abstract

Metal-halide perovskites have become appealing materials for optoelectronic devices. While the fast advancing stretchable/wearable devices require stability, flexibility and scalability, current perovskite still suffers from ambient-environmental instability and incompatible mechanical properties. To break the hindrance, recently perovskite–polymer composites have shown improved in-air stability with the assistance of polymers as the embedding media. However, their stability remains unsatisfactory in high-humidity environment or when immersed in water. These methods also suffer from limited processability with low yield (2D film or beads) and high fabrication cost (high temperature, air/moisture-free conditions), thereby limiting their device integration with complex structures and broader applications. Herein, by combining facile photopolymerization with room-temperature in-situ perovskite reprecipitation at low energy cost, a one-step scalable method is developed to produce freestanding highly-stable luminescent

organogels, within which $\text{CH}_3\text{NH}_3\text{PbBr}_3$ nanoparticles (NPs) are homogeneously distributed,. The perovskite-organogels present a record-high stability, maintaining their high quantum yields for > 110 days immersing in water at different pH and temperatures. This paradigm is universally applicable to broad choices of polymers, hence casting these emerging luminescent materials to a wide range of mechanical properties tunable from rigid to elastic. With intrinsically ultra-stretchable photoluminescent organogels, flexible LED devices were demonstrated with > 950% elongation. Rigid perovskite gels, on the other hand, permitted the deployment of 3D-printing technology to fabricate arbitrary 2D/3D luminescent architectures.

The thesis of Yucheng Zhang is approved.

Jenn-Ming Yang

Qibing Pei

Ximin He, Committee Chair

University of California, Los Angeles

2019

Table of Content

List of Figures.....	vi
List of Tables.....	vii
Acknowledgement.....	ix
1.Published Work.....	1
1.1 Abstract.....	1
1.2 Introduction.....	2
1.3 Results and Discussion.....	5
1.4 Experimental Section.....	16
1.6 Supporting Information	18
1.7 Reference	26

List of Figures

Figure 1. a) Schematic of the preparation of PNP gels, based on an on-site reprecipitation process. b, c) Photos of luminescent poly(butyl acrylate) (PBA) gel containing MAPbBr₃ NPs at, respectively, b) 5 minutes and c) 4 hours after taking out from toluene. d, e) The scanning electron microscopic (SEM) images of d) interior surface and e) exterior surface of the luminescent PNP gels. f, g) The SEM images of f) interior surface and g) exterior surface of the PBA gels without PNPs, as the control samples prepared under identical condition. h) The XRD patterns of MAPbBr₃ in the PBA gel, in comparison with the standard patterns of pure PBA and MAPbBr₃.....6

Figure 2. a1) The photographs of the corresponding luminescent PNP gels (MAPbBr₃ NPs-at-PBA gels) under indoor light and a2) under 365 nm UV excitation in dark. The concentration of the PNPs in polymers in a1) and a2) tapers off from left to right. b1, b2, c1, c2) The comparison of photographs of the PBA gel with 2.4% PNPs before and after immersing in water at room temperature for 110 days. d) Normalized PL intensity of PNP gels in the matrix as a function of quantum dots molar ratio. e) The water resistance test of luminescent PNP gels immersed in 20 °C water and 60 °C water. f) The pH resistance of luminescent PNP gels at pH = 2, pH = 4 aqueous acid and pH = 9, pH = 12 aqueous alkali. The tested sample is PBA gels with 2.4% molar ratio of MAPbBr₃.....8

Figure 3. a) The chemical structures of a variety of acrylates used as monomers of PNP gels. They include 1) butyl acrylate (BA), 2) poly(ethylene glycol) methyl ether acrylate (Acryl-PEG), 3) ethyl acrylate (EA), 4) methyl acrylate (MA), 5) 1,6-hexanediol diacrylate (HDODA). b1) The photographs of such luminescent polymer gels under indoor light. b2) the photographs of gels under 365nm UV excitation in dark. c) The UV-vis absorption (red) and PL emission (green)

spectra of PNP gels. d) Stress-strain curves of above PNP gels except HDODA. e1, e2) The stretchable PBA-based PNP gels under indoor light and UV irradiation.....11

Figure 4. a) Graphic structure of the down-converter white-LED (WLED) device with a MAPbBr₃ NPs-at-PBA gel layer and red CdSe QDs-at-PMMA as converter layers on a blue LED to generate white light. b) The emission spectra of a WLED device with a picture of the emitting device in the inset (scale bar = 1 cm). c) The color gamut of the WLED device in CIE1931. d-f) 2D patterns and 3D structures of MAPbBr₃ NPs-at-HDODA gels printed by a DLP-based 3D printer: d1) 2D art characters ‘UCLA’, e1) ring and f1) 3D lattice structure under white light, and d2), e2) and f2) under UV light respectively.....13

Figure S1. The morphology of the NPs-at-PBA samples in a) room-temperature water, b) 60°C water, and c) aqueous alkali (pH=12) after 20 days. The samples are cut in half to create a new surface before immersing in water or solutions. The fracture surface is destroyed by both 60°C water and aqueous alkali, while the sample in water is unaffected.....22

Figure S2. PNPs-at-(PBA-co-PAM) (1:1) a) under room light, b) under UV light, and c, d) PNPs-at-PAM under room light, showing that PNPs embedded in relatively hydrophilic copolymer poly(acrylate-co-acrylamide) lost its PL drastically. With PAM copolymer, the system is no longer capable of generating PNPs homogeneous inside the structure.....23

List of Tables

Table S1. PNPs-concentration dependent photoluminescent properties of MAPbBr₃ NPs embedded in PBA. The NPs concentration is defined as the molar concentration of MAPbBr₃ in DMF. The narrow FWHMs within the range between 16-21 nm indicate pure light emitting. The

PL emission peak decreases obviously from 555 nm to 546 nm with a concentration drop from 2.4% to 0.2%.....	19
Table S2. Acrylate-monomer-dependent photoluminescence properties of MAPbBr ₃ NPs embedded in different polyacrylate gels.....	20
Table S3. The strain at break and Young’s modulus of PNP-embedded PBA, PEA, PMA, PAcryl-PEG and PHDODA. All the tested gels are able to restore their shapes to initial states after the stress is released until obvious cracks appear on the gels near strain at break.....	21
Table S4. The lead concentration in liquid water containing MAPbBr ₃ NPs-at-PBA by a plasma-atomic emission spectrometry. Five reference solutions with concentration of 10 ppm, 20 ppm, 30 ppm, 40 ppm and 50 ppm Pb ²⁺ are prepared by dissolving corresponding amount of PbCl ₂ in water.....	24
Table S5. Comprehensive comparisons between this work and previous work including stability in water, reaction conditions and potential applications.....	25

Acknowledgement

This thesis is published in the journal of *Advanced Materials*. The ORCID identification number(s) for the author(s) of this article can be found under

<https://doi.org/10.1002/adma.201902928>.

Yucheng Zhang and Yusen Zhao contributed equally to this work. The authors thank the help from Yunzhe Qiu for the use of spectrometer. We acknowledge the support from the NSF Grant 1724526, the AFOSR Grant FA9550-17-1-0311, the ONR Award N000141712117, the Hellman Fellows Funds, and the UCLA Faculty Career Development Award from the University of California, Los Angeles.

Homogeneous Freestanding Luminescent Perovskite Organogel with Superior Water Stability

Keywords: perovskite quantum dots, stability, organogel, photoluminescent

Abstract

Metal-halide perovskites have become appealing materials for optoelectronic devices. While the fast advancing stretchable/wearable devices require stability, flexibility and scalability, current perovskite still suffers from ambient-environmental instability and incompatible mechanical properties. To break the hindrance, recently perovskite–polymer composites have shown improved in-air stability with the assistance of polymers as the embedding media. However, their stability remains unsatisfactory in high-humidity environment or when immersed in water. These methods also suffer from limited processability with low yield (2D film or beads) and high fabrication cost (high temperature, air/moisture-free conditions), thereby limiting their device integration with complex structures and broader applications. Herein, by combining facile photo-polymerization with room-temperature in-situ perovskite reprecipitation at low energy cost, a one-step scalable method is developed to produce freestanding highly-stable luminescent organogels, within which $\text{CH}_3\text{NH}_3\text{PbBr}_3$ nanoparticles (NPs) are homogeneously distributed,. The perovskite-organogels present a record-high stability, maintaining their high quantum yields for > 110 days immersing in water at different pH and temperatures. This paradigm is universally applicable to broad choices of polymers, hence casting these emerging luminescent materials to a wide range of mechanical properties tunable from rigid to elastic. With intrinsically ultra-stretchable photoluminescent organogels, flexible LED devices were demonstrated with > 950% elongation. Rigid perovskite

gels, on the other hand, permitted the deployment of 3D-printing technology to fabricate arbitrary 2D/3D luminescent architectures.

Introduction

Organometal halide perovskites have attracted extensive attention in the past decade owing to their excellent performance as active layers in photovoltaic devices.^[1] Also, their attractive intrinsic optical properties, such as bandgap tunability, long carrier lifetime, high photoluminescence quantum yield, and narrow emission linewidths,^[2] render them promising materials for display applications. Using perovskite quantum dots (PQDs) or perovskite nanoparticles (PNPs) including all-inorganic (e.g., CsPbX₃) and organic-inorganic (e.g., CH₃NH₃PbX₃) ones, a broad range of high-performance solar cells,^[3] light emitting diodes (LED),^[4] lasing,^[5,6] waveguides,^[7] photodetectors,^[8,9] and field effect transistors^[10] have been developed in recent years.

Accompanied by the excellent performance of PNPs come the undesirable material stability issues. The low formation energy of the material and highly mobile ionic structure with surface traps^[11] make perovskites vulnerable to external factors including light, moisture, and temperature. The poor stability has become the major obstacle for the practical application of PQDs-based solar cells, LEDs and other devices, whose performance often drop drastically, down to a few hours in ambient environment.^[12] Moreover, traditional device fabrication and testing utilize pre-formed PNPs, which require oxygen/moisture-free environment^[13] and high temperature^[14] for synthesis and post-annealing treatment, associated with high energy consumption. Addressing these instability issues, while maintaining the versatile processibility of these perovskite nanomaterials, may offer tremendous opportunities to optoelectronics and energy science. It is highly desirable to

achieve **in-situ and simultaneous** formation and protection of PNPs in a **one-pot synthesis** (where PNPs are formed being protected), which is suitable for large-scale industrial manufacturing with a low energy cost.

Recently many strategies have been explored for stabilizing the perovskite materials exposed to various harsh environments. For instance, surface modification including Shape-preserving transformation,^[15] oligomeric ligand functionalization,^[16] and silica matrix encapsulation^[17] have been reported to improve the stability, but PNPs in those demonstrations are not fully water resistant. Dense water-proof polymers, such as polystyrene, were used to encapsulate and protect PNPs against moisture. Also, fluorescent polymer composites with lanthanide ions, organic dyes or quantum dots (QDs) as the fluorescence centers have been broadly used in biosensing and optoelectronic devices. Embedding PNPs into the polymer matrix is a mutually beneficial process: the polymer matrix provides a protective structure to PNPs, and the PNPs endows the polymers with excellent optical properties, especially photoluminescent functions. In a recent report, a swelling–deswelling strategy was used to introduce pre-synthesized PNPs into spincoated polymer thin films to form the perovskite–polymer luminescent composites,^[18] which enabled stable photoluminescence (PL) in water for two months. However, the spin-coating process limits the composite as 2D planar films. Such processing inflexibility severely restricts the applications of such luminescent polymers. More importantly, this two-step swelling-deswelling method resulted in perovskite dispersion in only a few μm thin surfacial region of the polymer film, yielding an inhomogeneous material containing a thin PNPs-rich layer that occupies <10% of the entire polymer film thickness. Such a small fraction of active PNP layer in the polymer film limited the device efficiency. To overcome these disadvantages, PNPs-embedded nanoscale polymer beads^[19] were fabricated using the same swelling-deswelling method; however, the long-term water

resistance was compromised undesirably, with a >50% PL-intensity drop within only one week. So far there is still no effective method to endow perovskite materials with both high water resistance and flexibility (*i.e.*, structure designability and mechanical property tunability) at the same time. The increasing demands on various flexible or wearable optoelectronic devices, such as stretchable OLEDs^[20] necessitate the development of new perovskite materials with high stability and flexibility more urgent.

Compared to the previously used conventional polymer,^[12,13] crosslinked polymers or gels can provide a more favorable 3D compact matrix to protect the embedded PNPs, by directly forming freestanding and scalable structure.^[21] However, the intrinsic hydrophilicity of the conventional hydrogel system is incompatible to perovskites due to their sensitivity to moisture. Synthesis of PNPs in a gel matrix in a facile, scalable, and environment-stable manner has still not been realized.

Here, a homogeneous luminescent polymer organogel containing organic-inorganic PNPs, termed PNP gels, with record-high water resistance is reported. Inspired by the facile room-temperature PNP reprecipitation technique^[22,23] and benefiting from the porous structure of polymer gels, we successfully developed a fast one-pot photopolymerization method for synthesizing luminescent polyacrylate organogels, which possess high quantum efficiency and excellent mechanical properties tunable from a highly stretchable gel of 950% elongation to a highly rigid gel of a 110 MPa modulus. The polymer organogels can be immersed in water and aqueous acid solution with no apparent PL quenching for more than three months. Practically, the high stability and designability allow the perovskite materials to successfully construct flexible LED devices with high efficiency and long-term durability. Furthermore, the simple photopolymerization process also makes the perovskite polymer 3D-printable. This new 3D printing ability opens up enormous

opportunities for fabricating luminescent materials of arbitrary, complex 3D architectures, and rapid low-cost manufacturing of optoelectronic devices with previously unachievable structures.

Results and Discussion

The matrix of the PNP gels is a crosslinked hydrophobic polymer with a porous network microstructure that possesses the freestanding nature and good elastic properties of the gel.^[24] Instead of using traditional hydrophilic networks as in hydrogels, we selected hydrophobic polyacrylate as the matrix to embed and protect PNPs against ambient stress like moisture or general aqueous media. **Figure 1a** schematically shows the one-pot preparation of perovskite gels based on an on-site reprecipitation process. Specifically, to form an exemplary $\text{CH}_3\text{NH}_3\text{PbBr}_3$ NP-embedded poly (butyl acrylate) (PBA) gel, $\text{CH}_3\text{NH}_3\text{Br}$ (MABr) and PbBr_2 are dissolved into dimethylformamide (DMF) solvent at a 3:1 molar ratio with oleic acid (OA) and oleylamine (OAm) as the ligands to form the perovskite precursor (solution A). Then, the acrylate precursor (solution B) is prepared by mixing acrylate monomer with the crosslinker N,N'-methylenebisacrylamide (BIS) and the photo-initiator 2-Hydroxy-2-methylpropiophenone (Darocur 1173). By mixing the solution A and solution B, the PNP gel precursor is formed and can be photo-polymerized under UV light exposure into a transparent gel of desirable shape in a mold or by photolithographic 3D printer. Subsequently, the gel is immersed in toluene for solvent substitution. As the toluene gradually diffuses into the gel through those micro-pores, the gel swells for about twice in volume and the perovskite crystals start to nucleate and grow inside the gel matrix, due to the low solubility of the perovskite in toluene. Gradually, the color of the gel changes from transparent clear to opaque yellow-orange (Figure 1b). The as-obtained gel is dried in air for 4 hours to remove the

solvent. During the solvent evaporation, the swollen and sticky gel shrinks back to the original size with a robust and rigid mechanical strength, indicating the completion of formation of a strong luminescent PNP gel composite (Figure 1c). The fabrication method of this luminescent PNP gels has been found to be facile and robust without the need of harsh condition, such as vacuum or high temperatures required in traditional methods. The entire gel preparation process is conducted in ambient condition under room temperature, with no additional protection or treatment.

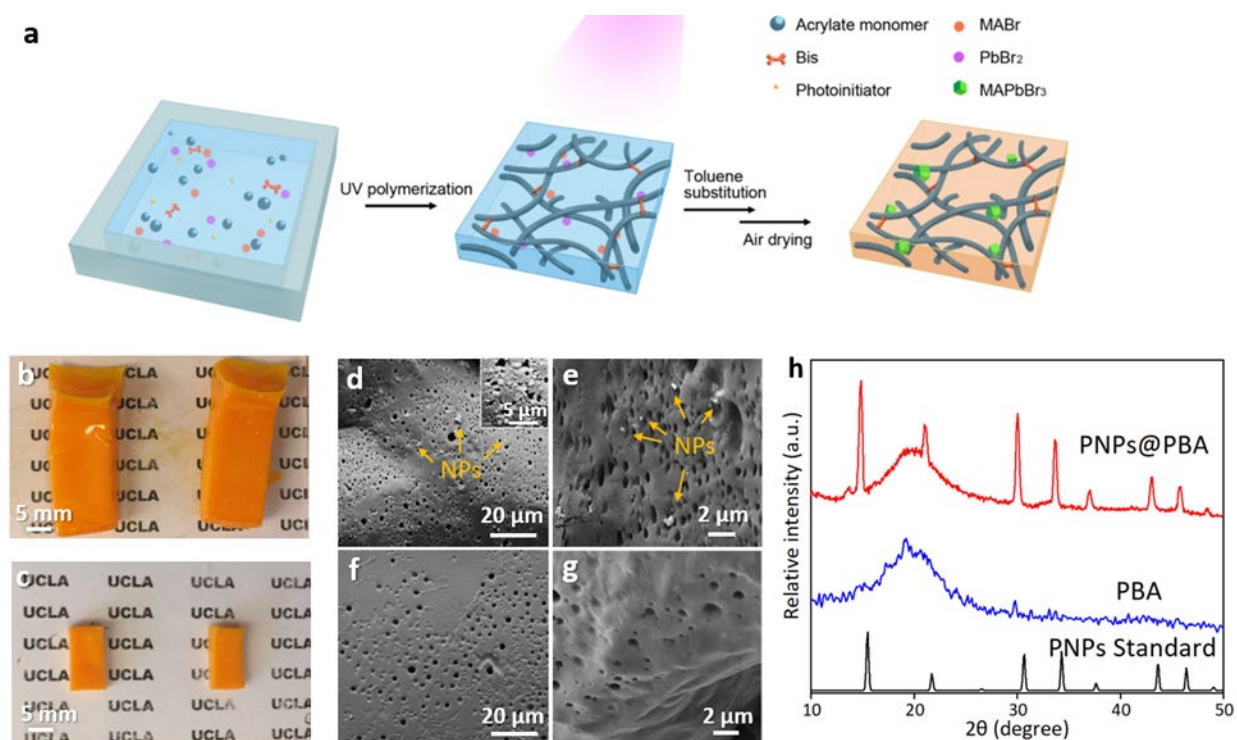


Figure 1. a) Schematic of the preparation of PNP gels, based on an on-site reprecipitation process. b, c) Photos of luminescent poly(butyl acrylate) (PBA) gel containing MAPbBr₃ NPs at, respectively, b) 5 minutes and c) 4 hours after taking out from toluene. d, e) The scanning electron microscopic (SEM) images of d) interior surface and e) exterior surface of the luminescent PNP gels. f, g) The SEM images of f) interior surface and g) exterior surface of the PBA gels without

PNPs, as the control samples prepared under identical condition. h) The XRD patterns of MAPbBr₃ in the PBA gel, in comparison with the standard patterns of pure PBA and MAPbBr₃.^[25]

Structural characterizations provide proofs that the PNPs are well dispersed throughout the entire 3D network of the gel. Scanning electron microscopy (SEM) images of both the surface and the internal structure of a typical gel with and without PNPs respectively are shown in Figure 1d-g. Both gels display identical typical porous structure, indicating that the embedding of NPs does not affect the morphology of the gel. Figure 1d and 1e show the PNP gels contain nanoparticles of ~100 nm diameter. By contrast, in the pristine PBA gel no such NPs is observed (Figure 1f, g). To verify the spatial distribution of the PNPs throughout the network, the interior cross-section of freshly cut PNP gels is imaged. As revealed by the morphology of the exterior and the interior surfaces of PNP gels respectively in Figure 1d and 1e, the PNPs are both uniformly dispersed in the gel matrix, suggesting the good protection of PNPs from the polymer matrix.

To further prove the encapsulation of PNPs in the polymer matrix and test the water stability of PNPs, the XRD pattern of the MAPbBr₃ NPs-at-PBA gel after immersion in water for 40 days is compared with those of the pure PBA and MAPbBr₃, as shown in Figure 1h. The pattern of MAPbBr₃ NPs-at-PBA gel has a baseline similar to the blank PBA gel and peaks corresponding to the standard pattern of MAPbBr₃. This proves the encapsulation of PNPs in the polymer matrix with high water stability.

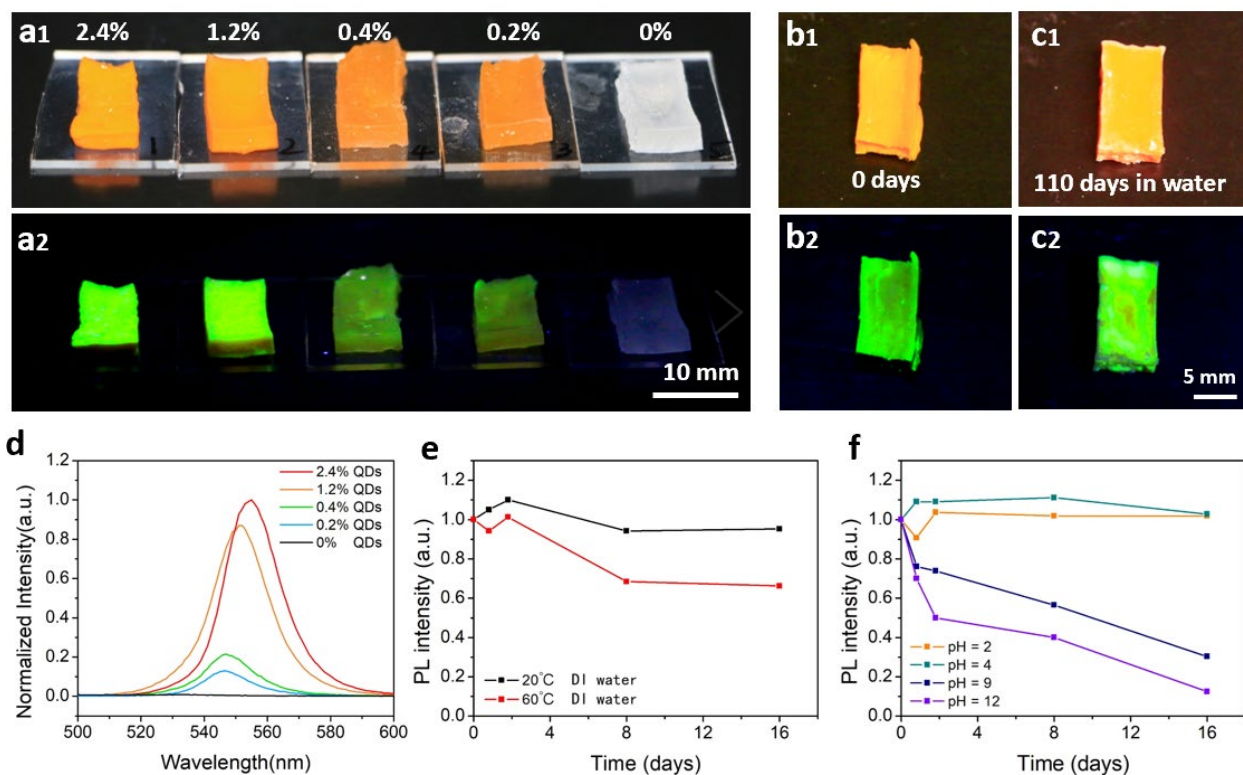


Figure 2. a1) The photographs of the corresponding luminescent PNP gels (MAPbBr₃ NPs-at-PBA gels) under indoor light and a2) under 365 nm UV excitation in dark. The concentration of the PNPs in polymers in a1) and a2) tapers off from left to right. b1, b2, c1, c2) The comparison of photographs of the PBA gel with 2.4% PNPs before and after immersing in water at room temperature for 110 days. d) Normalized PL intensity of PNP gels in the matrix as a function of quantum dots molar ratio. e) The water resistance test of luminescent PNP gels immersed in 20 °C water and 60 °C water. f) The pH resistance of luminescent PNP gels at pH = 2, pH = 4 aqueous acid and pH = 9, pH = 12 aqueous alkali. The tested sample is PBA gels with 2.4% molar ratio of MAPbBr₃.

The photoluminescent performance of the PNP gels has been examined. A series of PNP gels made from precursor solutions of different MAPbBr₃ concentrations in DMF are measured, to study the influence of PNP-precursor concentration on the PL intensity (**Figure 2a1, a2**). As expected, the PL intensity of the PNP gel increases with the concentration of PNP precursor. The PL intensity change as a function of concentration is nonlinear, perhaps because the formation of PNPs in the gel is accompanied by the diffusion of toluene, taking away some PNPs (Figure 2d). Another noteworthy phenomenon is the redshift with a higher concentration PNP precursor solution; this could arise primarily from the self-absorption of emitted photons known for high-perovskite-concentration materials.^[26]

Many previous works managed to improve the stability of PNPs in ambient air but failed to maintain the PL when in direct contact with liquid water.^[27] Here encapsulating PNPs with the hydrophobic polyacrylate matrices successfully lead to ultrahigh stability of the PNPs when exposed to ambient environment with high humidity and even when immersed in aqueous solutions. By contrast, PNPs embedded in relatively hydrophilic copolymer poly(acrylate-co-acrylamide) immersed in RT water lost its PL drastically in a control test (Figure. S2), which also indirectly proved the effect of hydrophobicity on protecting PNPs from water. To systematically examine its chemical- and thermal-stability when immersed in water, the PL intensity change of PNP gels as a function of time was monitored by measuring the PL spectra of the gels immersed in various aqueous systems during the period of 16 days, including deionized (DI) water (pH=7) at room temperature (RT) and elevated temperature (60°), hydrochloric acid solutions (pH=2 and pH=4), and sodium hydroxide (NaOH) solutions (pH=9 and pH=12). As shown in Figure 2e, f, the PNP gels exhibited excellent intensity retention of 95.3% in water and 102% in acid solution of pH = 12 under room temperature for 16 days. Surprisingly, the PL intensity even increased for RT

water in the first few days and for an acidic solution, probably attributed to the photo enhancement, a typical phenomenon reported both in traditional nanoparticles and perovskite nanoparticles.^[28] In the long-term stability test, we further found that the PL properties of the PNPs gels were well-maintained after immersing in RT water for more than 110 days, as shown in Figure 2b1, b2, c1, c2. A distinct PL quenching for samples in 60 °C water and aqueous alkali was observed after 16 days, with the one in pH=12 aqueous alkali showing the most PL intensity reduction. Such a loss of PL intensity was found to arise from the long-term thermal- and alkali-instability of PBA, as verified by the clear morphology change of the samples immersed in RT water, 60° water, and aqueous alkali for 20 days as shown in **Figure S1**. The fracture surfaces of the latter two samples have been severely corroded by high-temperature or high-alkali aqueous environment, in contrast to the intact surface of the sample immersed in RT DI water. Thus, the corroded polymer matrix no longer provides hydrophobic protection for PNPs encapsulated in the matrix, which leads to the PL quenching.

The traditional lead-containing perovskite, due to the hydrolysis of lead in aqueous environment, suffers from severe toxicity issues and limited applications in biomaterials and biomedical fields. Hence, beyond the presented promising long-term stability of the PNP gels, we examined the lead content changes in water before and after immersing the gels, using plasma-atomic emission spectrometry (ICP-AES). The aqueous phases after gel immersion for 1 day and 20 days, respectively, have Pb²⁺ concentrations of 0.677 ppm and 0.749 ppm, comparable to 0.663 ppm of blank DI water and well below the safe value of Pb²⁺ (1.931 ppm) for bioimaging applications.^[13] This lead leaking test based on the Pb²⁺ concentration in the immersion liquids provides another proof for the firm encapsulation of PNPs in the polymer matrix and the superior water resistivity.

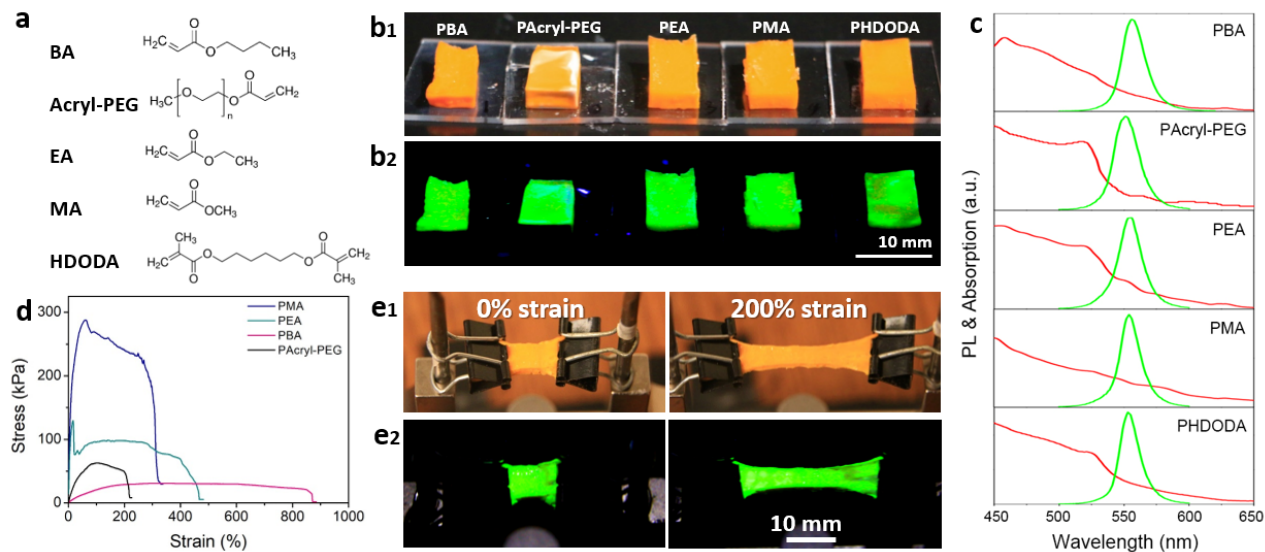


Figure 3. a) The chemical structures of a variety of acrylates used as monomers of PNP gels. They include 1) butyl acrylate (BA), 2) poly(ethylene glycol) methyl ether acrylate (Acryl-PEG), 3) ethyl acrylate (EA), 4) methyl acrylate (MA), 5) 1,6-hexanediol diacrylate (HDODA). b1) The photographs of such luminescent polymer gels under indoor light. b2) the photographs of gels under 365nm UV excitation in dark. c) The UV-vis absorption (red) and PL emission (green) spectra of PNP gels. d) Stress-strain curves of above PNP gels except HDODA. e1, e2) The stretchable PBA-based PNP gels under indoor light and UV irradiation.

To demonstrate the universal applicability of our method for preparing luminescent PNP gels, a variety of luminescent PNP gels have been successfully synthesized using a series of acrylates as monomers (**Figure 3a**), including butyl acrylate (BA), poly(ethylene glycol) methyl ether acrylate (Acryl-PEG), ethyl acrylate (EA), methyl acrylate (MA), 1,6-hexanediol diacrylate (HDODA). As shown in Figure 3b1, b2, the PNP gels are all in orange-yellow color under room light (Figure 3b1) and appear bright green under UV excitation throughout the entire body of the material (Figure

3b2), indicating high homogeneity of these composite materials. The PL emission wavelength in the range of 551-555 nm matches very well with the absorption onset wavelength located in the same range (Figure 3c). The full widths at half maximum (FWHM) of those gels are as narrow as 17-22 nm, which indicates the high purity of the generated green color. This narrow FWHM level outperforms the perovskite-polymer composite films prepared through the MAPbBr₃-polymer precursor mixture approach^[29] (>30 nm) and through the swelling-deswelling approach (18-24 nm).^[12]

Besides having excellent photoluminescent energy conversion efficiency, luminescent materials that can undergo large deformation, *i.e.*, good tensile property, are highly desired especially for stretchable LEDs and many other flexible devices. On the other hand, a decent Young modulus, instead, would be required for realizing 3D printing of complex luminescent structures. We have successfully realized this wide range of mechanical properties by designing a series of PNP gels with different polymer chain lengths, as their stress-strain curves shown in Figure 3d. As expected, the breaking elongation increases with the alkyl chain length. In the case of poly(butyl acrylate), the elongation at break exceeds 850%, while for poly(ethyl acrylate) and poly(methyl acrylate), the values are 468% and 322% respectively. This alkyl pendant-chain-length dependency of the breaking elongation is because longer pendant groups tend to limit the close chains to pack and increase the rotational mobility of the polymer chain,^[30] resulting in the enhanced flexibility and stretchability of the overall gel network. Oppositely, lower alkyl pendant chain leads to higher Young's modulus but lower the tensile property. Using the PBA gel as a demonstration, we further examined the luminescent performance of PNP gels under reversible stretching (200% strain) and recovery (Video S1). Figure 3e shows photographs of a PBA-based PNP gel without stretching and at 200% strain. The stretched PNP gel presented uniform and bright illumination throughout

the entire exposed area. With the demonstrated capability of making PNP gels with a broad spectrum of mechanical properties, from high stretchability to high strength, and luminescent properties under reversible stretching, this method serves as a broad-based platform for rational design of stretchable luminescent devices.

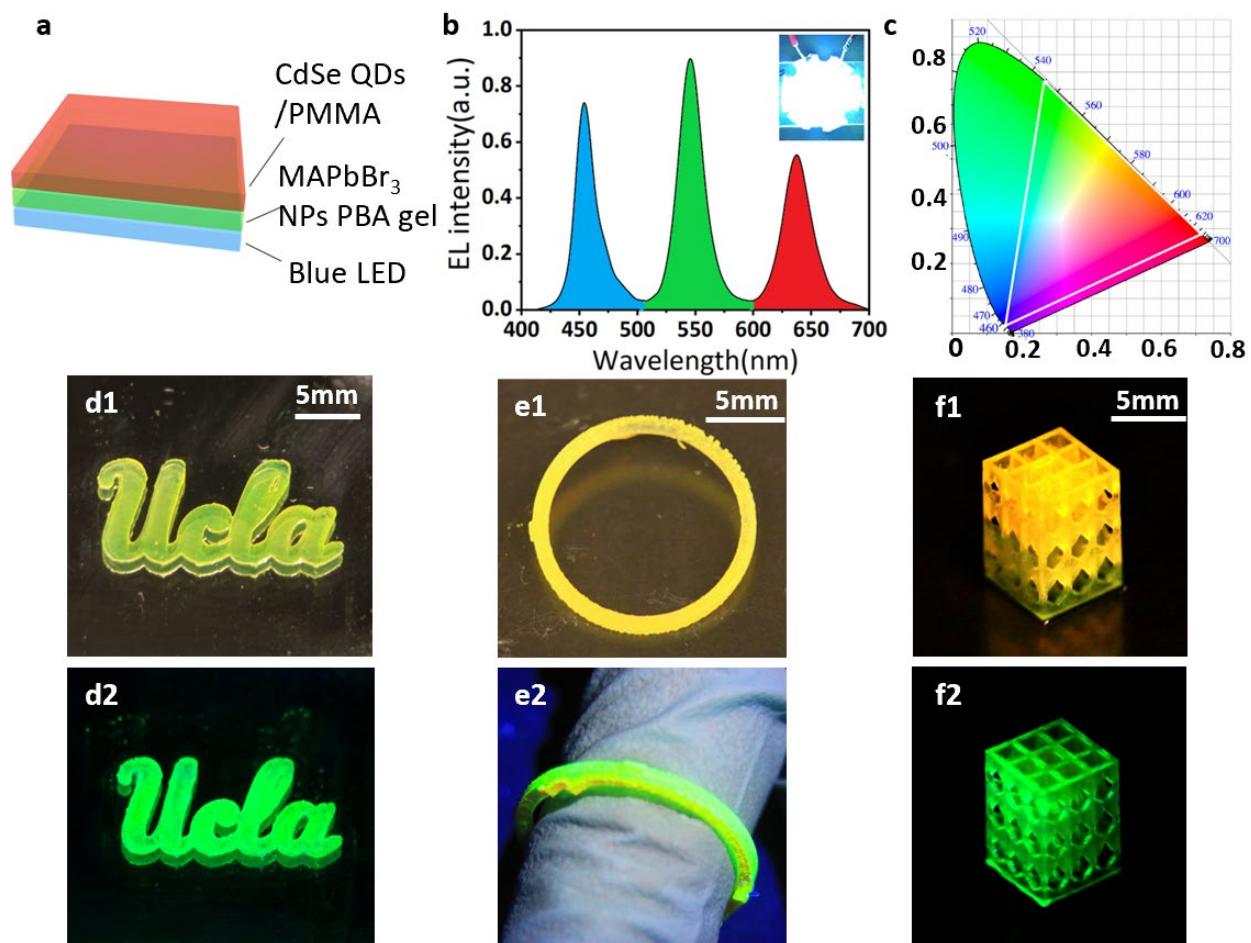


Figure 4. a) Graphic structure of the down-converter white-LED (WLED) device with a MAPbBr₃ NPs-at-PBA gel layer and red CdSe QDs-at-PMMA as converter layers on a blue LED to generate white light. b) The emission spectra of a WLED device with a picture of the emitting device in the inset (scale bar = 1 cm). c) The color gamut of the WLED device in CIE1931. d-f) 2D patterns and

3D structures of MAPbBr₃ NPs-at-HDODA gels printed by a DLP-based 3D printer: d1) 2D art characters 'UCLA', e1) ring and f1) 3D lattice structure under white light, and d2), e2) and f2) under UV light respectively.

Based on the high stability, color purity and material versatility, these luminescent materials with green color can be readily assembled as the down converter in the white-light LED (WLED) devices, where a blue LED pumps the red and green phosphor layers to generate white light (**Figure 4a**). As a simple demonstration, a PNP gel film and a red CdSe-at-PMMA film were deposited on a blue LED emitting at wavelength 454 nm with FWHM 20 nm, generating corresponding green light at wavelength 545 nm with FWHM 24 nm and red light at wavelength 637 nm with FWHM 29 nm and the resulted white light from a mixture of three primary colors as shown in Figure 4b. The spectral locus coordinates are (0.15, 0.021) as the bright blue color, (0.27, 0.72) as the emerald green color, and (0.71, 0.28) as the super red color are shown in Figure 4c, presenting great potentials for white-light-emitting devices. Additionally, the great stretchability with full mechanical reversibility of the luminescent PNP gels allows them to be alternative options to stretchable light emitting diodes.

Previous works focusing on the enhancement of stability of PNPs either encapsulate PNPs at the surface of polymer thin film through spin coating fabrication,^[15] or wrap pre-made NPs within polymer beads forming luminescent powders.^[16] These complex fabrication procedures and the lack of substrates options in these methods severely limit the PNP composites to 2D structures or even lower dimensions. Compared to those restricted luminescent structures, the presented PNP gels can not only be prepared into the conventional 2D film devices as demonstrated in the WLED

device, but also be fabricated into arbitrary complex 3D structures by 3D printing in a high-precision and time-effective fashion, giving credit to the simple photo-polymerization and the (solvent-induced) on-site reprecipitation process. Figure 4d-f showcases several examples of 2D patterns (Figure 4d1, d2) and 3D structures (Figure 4e1, e2, f1, f2) of printed luminescent gels using projection micro-stereolithography (P μ SL). The favorable mechanical properties especially the rigidity, the low swelling ratio and the ease of photopolymerization of PHDODA make it a qualified material for nearly all digital light processing (DLP)-based 3D printings. The combination of the new luminescent gel with 3D printing techniques opens the opportunities for preparing luminescent materials with arbitrary solid patterns and structures.

In summary, we have established a convenient and universal one-pot synthesis strategy to achieve ultrahigh water stability and tunable mechanical properties of perovskites, by in-situ producing and embedding perovskite quantum dots into the hydrophobic polyacrylate matrix. This low-energy-cost strategy uses the facile room-temperature PNP reprecipitation technique with UV polymerization to obtain a photoluminescent gel with homogeneously distribute PNPs, which maintaining the PL in water for more than three months. Fundamentally, this study has also advanced the understanding of perovskite stability and protection under various environmental conditions. The generality of our method and the modularity of the material design provide ample choices of polyacrylate or other gels with different mechanical properties, as well as various PNPs such as MAPbCl₃. To demonstrate the tunable mechanical properties (from elastic to rigid), a highly stretchable perovskite-based WLED devices and several 3D-printed freestanding architectures were fabricated. Overall, this new method successfully enhanced the perovskite stability without compromising the processability and scalability as the expense, which has never been realized previously. All these resulted in improvement of the overall (photo)electrical

properties of perovskite materials, we believe this new kind of stable photoluminescent gels has huge potential in broad applications of optoelectronic devices.

Experimental Section

Fabrication of the photoluminescent gel with MAPbBr₃ NPs in polyacrylate, using PBA as

an example: Precursor solution A was prepared by dissolving 3 mmol MABr and 1 mmol PbBr₂ into 15 ml DMF, with 1.5 ml OA and 60 μ l OAm as ligands. The precursor A was then heated at 80 °C for 10 minutes under stirring. Precursor solution B was prepared by dissolving 10 mg BIS and 5 μ l Darocur 1173 into 5.6 mmol BA (same mole amount monomer for MA, EA and Acryl-PEG, 2.8mmol for HDODA). 0.6 ml of precursor A was added to 0.8 ml of precursor B (0.520 ml for MA, 0.610 ml for EA, 0.630 ml for Acryl-PEG, and 0.420 ml for HDODA), and the mixture was injected to the designed model as a container for UV photo-polymerization. Both two precursors were proved to be valid after 60 days storage under dark and 4 °C. A colorless gel was obtained by exposing the mixture of A and B under UV chamber for 180 seconds. The gel with PNPs was obtained by immersing the gel into toluene for at least 2 hours and drying in the air for 4 hours.

Characterizations: Scanning electron microscope characterizations were carried out with SUPRAU 40VP Field Emission Scanning Electron Microscope (ZEISS Supra 40VP SEM). All samples were coated with Au before test without further treatments.

X-ray diffraction $2\theta:\omega$ scans were performed on a Bede high resolution X-ray diffractometer with a copper radiation source.

Steady-state photoluminescence (PL) spectra were obtained using Horiba Jobin Yvon system with some structural modification on sample loading part with excitation wavelength at 450 nm. All the measurements were carried out at room temperature.

The elongation-at-break test and Young's modulus measurement were conducted on the DMA (TA Instruments, Q800) at room temperature. The samples are the polyacrylate gels with PNP concentrations as mentioned above.

The emission spectra was characterized via a CCS 200 compact spectrometer.

3D printing process: A custom-built DLP-based 3D printer was used to print the 2D patterns and 3D structures of PNP gels in this work. The system consists of a PRO4500 UV light (385 nm) projector (Wintech Digital System Technology Corporation), a motorized translation stage mounted to a motor controlled (Thorlabs, Inc.) and a computer program to control the system. The resolution of the 3D printer can achieve 30 μm on the x-y plane and 10 μm in the z-axis direction.

The 2D patterns as shown in the paper were one-step printed by projecting the light pattern for 15 seconds. For the ring structure and the 3D lattice structure, their CAD 3D models were firstly constructed and then sliced into serials of 2D images. The structures were printed layer by layer. Each layer was cured for 15 seconds. After printing, the samples were rinsed with toluene to precipitate the quantum dots trapped inside the polymers.

Homogeneous freestanding luminescent perovskite organogel with superior water stability

Supporting Information

Table S1. PNPs-concentration dependent photoluminescent properties of MAPbBr₃ NPs embedded in PBA. The NPs concentration is defined as the molar concentration of MAPbBr₃ in DMF. The narrow FWHMs within the range between 16-21 nm indicate pure light emitting. The PL emission peak decreases obviously from 555 nm to 546 nm with a concentration drop from 2.4% to 0.2%.

NPs concentration (mole%)	2.4	1.2	0.4	0.2	0
Normalized PLQYs (%)	100	87.1	21.5	12.9	0
FWHM (nm)	20	21	17	16	/
PL emission peak (nm)	555	551	547	546	/

Table S2. Acrylate-monomer-dependent photoluminescence properties of MAPbBr₃ NPs embedded in different polyacrylate gels.

Acrylate gel	PBA	PAcryl-PEG	PEA	PMA	PHDODA
FWHM (nm)	20	17	21	18	22
PL emission peak (nm)	555	553	554	554	551

Polymer gel	PBA	PEA	PMA	PAcryl-PEG	PHDOD
Strain at break (%)	870	468	322	219	/
Young's modulus (MPa)	/	0.8	0.8	0.12	110

Table S3. The strain at break and Young's modulus of PNP-embedded PBA, PEA, PMA, PAcryl-PEG and PHDODA. All the tested gels are able to restore their shapes to initial states after the stress is released until obvious cracks appear on the gels near strain at break.

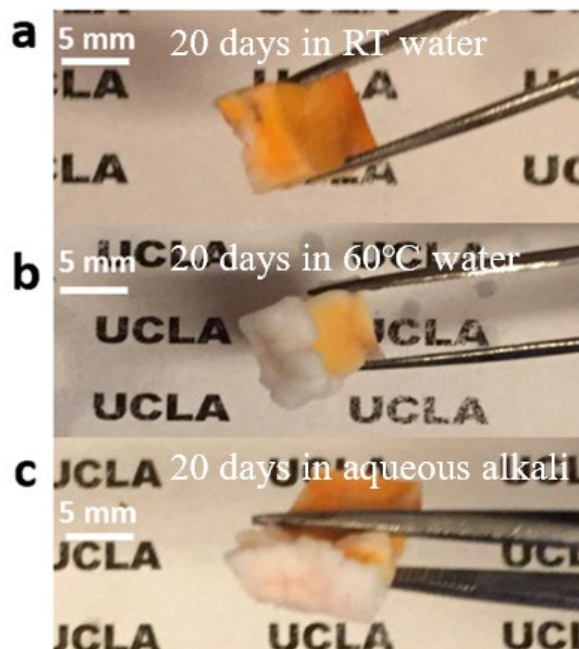


Figure S1. The morphology of the NPs-at-PBA samples in a) room-temperature water, b) 60°C water, and c) aqueous alkali (pH=12) after 20 days. The samples are cut in half to create a new surface before immersing in water or solutions. The fracture surface is destroyed by both 60°C water and aqueous alkali, while the sample in water is unaffected.

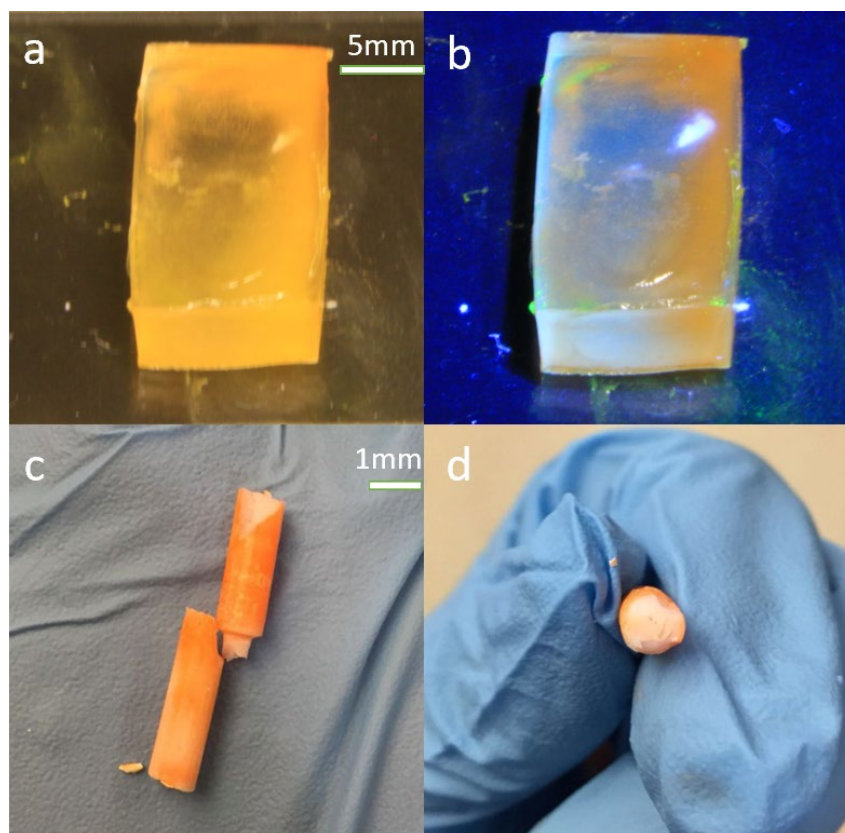


Figure S2. PNPs-at-(PBA-co-PAM) (1:1) a) under room light, b) under UV light, and c, d) PNPs-at-PAM under room light, showing that PNPs embedded in relatively hydrophilic copolymer poly(acrylate-co-acrylamide) lost its PL drastically. With PAM copolymer, the system is no longer capable of generating PNPs homogeneous inside the structure.

Sample	Pb 216.999 Quant Average (mg/L)	Pb 220.353 Quant Average (mg/L)	Pb 405.783 Quant Average (mg/L)
Liquid water contains NPs@PBA for 24 hours	0.768	0.677	0.890
Liquid water contains NPs@PBA for 20 days	0.786	0.749	0.794

Table S4. The lead concentration in liquid water containing MAPbBr₃ NPs-at-PBA by a plasma-atomic emission spectrometry. Five reference solutions with concentration of 10 ppm, 20 ppm, 30 ppm, 40 ppm and 50 ppm Pb²⁺ are prepared by dissolving corresponding amount of PbCl₂ in water.

Table S5. Comprehensive comparisons between this work and previous work including stability in water, reaction conditions and potential applications.

	Stability in water	Reaction temp.	Energy cost, fab. time	Reaction environment	Printable 3D structure	Stretchable (strain)
This work	✓	Room temp.	UV, 2 mins	Ambient	✓	>850%
Ref 1	✗	75°C	UV, 12 hrs Heat, 12 hrs	Ambient	✗	<180%
Ref 2	✗	70°C	Heat, 10 hrs	N ₂	✗	✗
Ref 3	✗	Room temp.	E-spinning, 8 hrs	Ambient	✗	170%
Ref 4	✓	30-80°C	Heat, 2-8 hrs	Glove box	✗	✗
Ref 5	✓	85-100°C	Heat, 8 hrs	Glove box	✗	✗

References

Manuscript:

- [1] W. Yin, J. Yang, J. Kang, Y. Yan, S. Wei, *Journal of Materials Chemistry A*. **2015**, 3.
- [2] P. Gao, M. Grätzel, M. Nazeeruddin, *Energy Environ. Sci.* **2014**, 7.
- [3] J. Xue, J.W. Lee, Z. Dai, R. Wang, S. Nuryyeva, M.E. Liao, S.Y. Chang, L. Meng, D. Meng, P. Sun, O. Lin, *Joule*. **2018**, 2
- [4] C. Sun, Y. Zhang, C. Ruan, C. Yin, X. Wang, Y. Wang, W. Yu, *Advanced Materials*. **2016**, 28.
- [5] S. Chen, K. Roh, J. Lee, W. Chong, Y. Lu, N. Mathews, T. Sum, A. Nurmikko, *ACS Nano* 2016, 10.
- [6] G. Xing, N. Mathews, S. Lim, N. Yantara, X. Liu, D. Sabba, M. Grätzel, S. Mhaisalkar, T. Sum, *Nature Materials* 2014, 13.
- [7] T. Cohen, T. Milstein, D. Kroupa, J. MacKenzie, C. Luscombe, D. Gamelin, *Journal of Materials Chemistry A* 2019, 7.
- [8] L. Zhou, K. Yu, F. Yang, J. Zheng, Y. Zuo, C. Li, B. Cheng, Q. Wang, *Dalton Transactions*. **2017**, 46.
- [9] L. Dou, Y. Yang, J. You, Z. Hong, W. Chang, G. Li, Y. Yang, *Nature Communications*. **2014**, 5
- [10] K. Wang, S. Dai, Y. Zhao, Y. Wang, C. Liu, J. Huang, *Small*. **2019**, 15.
- [11] A. Buin, P. Pietsch, J. Xu, O. Voznyy, A. Ip, R. Comin, E. Sargent, *Nano Letters*. **2014**, 14.
- [12] Y. Wei, Z. Cheng, J. Lin, *Chemical Society Reviews*. **2019**, 48.
- [13] M. Liu, M. Johnston, H. Snaith, *Nature* **2013**, 501.
- [14] A. Mei, X. Li, L. Liu, Z. Ku, T. Liu, Y. Rong, M. Xu, M. Hu, J. Chen, Y. Yang, M. Gratzel, H. Han, *Science* **2014**, 345
- [15] T. Holtus, L. Helmbrecht, H. Hendrikse, I. Baglai, S. Meuret, G. Adhyaksa, E. Garnett, W. Noorduyn, *Nature Chemistry*. **2018**, 10.
- [16] H. Huang, B. Chen, Z. Wang, T. Hung, A. Sussha, H. Zhong, A. Rogach, *Chemical Science*. **2016**, 7
- [17] C. Sun, Y. Zhang, C. Ruan, C. Yin, X. Wang, Y. Wang, W. Yu, *Advanced Materials*. **2016**, 28.

-
- [18] Y. Wang, J. He, H. Chen, J. Chen, R. Zhu, P. Ma, A. Towers, Y. Lin, A. Gesquiere, S. Wu, Y. Dong, *Advanced Materials*. **2016**, 28.
- [19] Y. Wei, X. Deng, Z. Xie, X. Cai, S. Liang, P. Ma, Z. Hou, Z. Cheng, J. Lin, *Advanced Functional Materials*. **2017**, 27.
- [20] S. Bade, X. Shan, P. Hoang, J. Li, T. Geske, L. Cai, Q. Pei, C. Wang, Z. Yu, *Advanced Materials*. **2017**, 29.
- [21] K. Gattás-Asfura, Y. Zheng, M. Micic, M. Snedaker, X. Ji, G. Sui, J. Orbulescu, F. Andreopoulos, S. Pham, C. Wang, R. Leblanc, *The Journal of Physical Chemistry B*. **2003**, 107.
- [22] Y. Niu, F. Zhang, Z. Bai, Y. Dong, J. Yang, R. Liu, B. Zou, J. Li, H. Zhong, *Advanced Optical Materials*. **2014**, 3.
- [23] F. Zhang, H. Zhong, C. Chen, X. Wu, X. Hu, H. Huang, J. Han, B. Zou, Y. Dong, *ACS Nano* 2015, 9.
- [24] L. Rogovina, V. Vasil'ev, E. Braudo, *Polymer Science Series C*. **2008**, 50.
- [25] A. Jaffe, Y. Lin, C. Beavers, J. Voss, W. Mao, H. Karunadasa, *ACS Central Science*. **2016**, 2.
- [26] Y. Fang, H. Wei, Q. Dong, J. Huang, *Nature Communications* 2017, 8.
- [27] H. Zhang, X. Wang, Q. Liao, Z. Xu, H. Li, L. Zheng, H. Fu, *Advanced Functional Materials*. **2017**, 27.
- [28] D. de, Quillettes, W. Zhang, V. Burlakov, D. Graham, T. Leijtens, A. Osherov, V. Bulović, H. Snaith, D. Ginger, S. Stranks, *Nature Communications* 2016, 7, DOI 10.1038/ncomms11683.
- [29] D. Di, K. Musselman, G. Li, A. Sadhanala, Y. Ievskaya, Q. Song, Z. Tan, M. Lai, J. MacManus-Driscoll, N. Greenham, R. Friend, *The Journal of Physical Chemistry Letters*. **2015**, 6.
- [30] "Factors Tg", can be found under <https://faculty.uscupstate.edu/llever/polymer%20resources/FactorsTg.htm> (accessed: April 2019).

supporting information:

- [1] Y. Xin, H. Zhao, J. Zhang, *ACS Applied Materials & Interfaces* **2018**, 10.
- [2] Y. Wei, X. Deng, Z. Xie, X. Cai, S. Liang, P. Ma, Z. Hou, Z. Cheng, J. Lin, *Advanced Functional Materials* **2017**, 27, DOI 10.1002/adfm.201770230.
- [3] C. Lin, D. Jiang, C. Kuo, C. Cho, Y. Tsai, T. Satoh, C. Su, *ACS Applied Materials & Interfaces* **2018**, 10.
- [4] Y. Wang, J. He, H. Chen, J. Chen, R. Zhu, P. Ma, A. Towers, Y. Lin, A. Gesquiere, S. Wu, Y. Dong, *Advanced Materials* **2016**, 28.
- [5] S. Raja, Y. Bekenstein, M. Koc, S. Fischer, D. Zhang, L. Lin, R. Ritchie, P. Yang, A. Alivisatos, *ACS Applied Materials & Interfaces* **2016**, 8.